

Electronic Supplementary Information (ESI)

# Synthesis of regioblock copolythiophene by Negishi catalyst-transfer polycondensation using $t\text{Bu}_2\text{Zn}\cdot 2\text{LiCl}$

Eisuke Goto,<sup>a</sup> Yuto Ochiai,<sup>a</sup> Chen-Tsyr Lo,<sup>a</sup> Tomoyuki Koganezawa,<sup>b</sup> Mitsuru Ueda<sup>a</sup>  
and Tomoya Higashihara\*<sup>a</sup>

<sup>a</sup>*Department of Organic Materials Science, Graduate School of Organic Materials  
Science, Yamagata University, 4-3-16 Jonan, Yonezawa, Yamagata 992-8510, Japan*

<sup>b</sup>*Japan Synchrotron Radiation Research Institute (JASRI), SPring-8, 1-1-1 Kouto,  
Sayo, Hyogo 679-5198, Japan*

## Corresponding Author

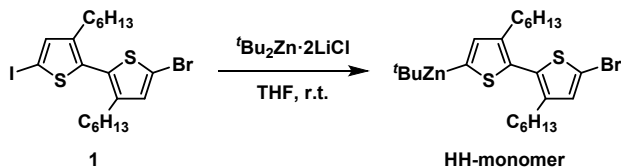
Tomoya Higashihara\* (E-mail: [thigashihara@yz.yamagata-u.ac.jp](mailto:thigashihara@yz.yamagata-u.ac.jp))

## **Table of contents**

Synthesis	3
$^1\text{H}$ and $^{13}\text{C}$ NMR spectra	6
SEC UV traces	11
Schematic illustrations	14
In-plane 1D GIWAXS profiles	15
2D GISAXS patterns	16
1D GISAXS profiles	17
TGA curves	18
DSC curves	19
UV-vis absorption	20
Reference	21

# Synthesis

## *Preparation of a THF solution of HH-monomer*



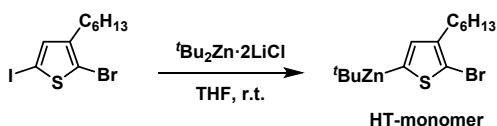
**Scheme S1.** Synthesis of HH-monomer by zinc-iodine exchange reaction

**Table S1.** Synthesis of HH-monomer by zinc-iodine exchange reaction using  $t\text{Bu}_2\text{Zn}\cdot 2\text{LiCl}$  under varied conditions.

Run	$[t\text{Bu}_2\text{Zn}\cdot 2\text{LiCl}]/[1]^a$	$[\text{LiCl}]/[1]^b$	Conc. (M) <sup>c</sup>	Conv. (%) <sup>d</sup>
S1	1.0	0	0.0242	61
S2	2.0	0	0.0213	0
S3	1.0	3.0	0.0239	37
3	1.0	0	0.107	95

<sup>a</sup> Initial molar ratio of  $t\text{Bu}_2\text{Zn}\cdot 2\text{LiCl}$  for **1**. <sup>b</sup> Initial molar ratio of LiCl for **1**. <sup>c</sup> Concentration (mol/L) of reaction mixture for synthesizing HH-monomer. <sup>d</sup> Conversion of zinc-iodine exchange reaction was evaluated by  $^1\text{H}$  NMR spectroscopy.

## *Preparation of a THF solution of HT-monomer as the second monomer*

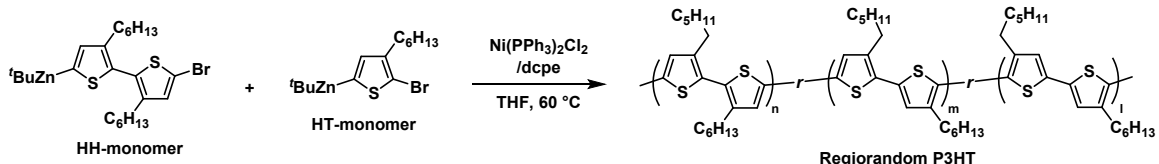


**Scheme S2.** Synthesis of HT-monomer by zinc-iodine exchange reaction

2-Bromo-3-hexyl-5-iodothiophene (185 mg, 0.496 mmol) was placed in a 5 mL two-necked flask purged with  $\text{N}_2$ . After dissolving 2-bromo-3-hexyl-5-iodothiophene in dehydrated THF (5 mL), a 0.184 M THF solution of  $t\text{Bu}_2\text{Zn}\cdot 2\text{LiCl}$  (2.7 mL, 0.50

mmol) was added and stirred at room temperature for 30 min to afford the HT-monomer.

### Synthesis of regiorandom P3HT



**Scheme S3.** Synthesis of regiorandom P3HT

**1** (112 mg, 0.207 mmol) and 2-bromo-3-hexyl-5-iodothiophene (154 mg, 0.413 mmol) were placed in a 20 mL two-necked flask purged with N<sub>2</sub>. After dissolving them in dehydrated THF (2 mL), a 0.184 M THF solution of *t*Bu<sub>2</sub>Zn·2LiCl (3.4 mL, 0.62 mmol) was added at 0 °C and stirred at room temperature for 1 h. Then, the reaction mixture was diluted with 10 mL of dehydrated THF. The Ni catalyst (0.0092 mmol) solution (5 mL), which was prepared in another batch by mixing Ni(PPh<sub>3</sub>)<sub>2</sub>Cl<sub>2</sub> (6.0 mg, 0.0092 mmol) and dcpe (9.7 mg, 0.023 mmol) in THF (5 mL), was added to start the polymerization. The polymerization was carried out at 60 °C for 30 min, followed by quenching with 5 M HCl aq. (2 mL). The quenched solution was extracted with chloroform, washed with water, and analyzed by SEC directly before precipitation. The crude solution was poured into a large amount of methanol/water (200 mL/100 mL) to precipitate the polymer. After filtrating and drying under

vacuum, the crude HHTT-P3HT was obtained as a dark red solid (91 mg, 66%). SEC:  $M_n = 11,200$ ,  $M_w/M_n = 1.46$ .  $^1\text{H}$  NMR (400 MHz, chloroform-*d*):  $\delta$  7.10-6.91 (m, 1H), 2.88-2.68 (m, 1H), 2.66-2.42 (m, 1H), 1.78-1.50 (m, 2H), 1.49-1.15 (m, 6H), 0.99-0.80 (m, 3H).  $^{13}\text{C}$  NMR (101 MHz, chloroform-*d*)  $\delta$  143.52, 143.00, 140.44, 140.02, 139.92, 137.11, 136.91, 135.82, 134.96, 133.89, 130.76, 130.62, 130.52, 129.75, 128.73, 128.44, 127.52, 127.28, 126.69, 125.94, 125.26, 31.99, 30.83, 30.66, 29.61, 29.41, 29.29, 22.93, 22.75, 14.27.

# <sup>1</sup>H and <sup>13</sup>C NMR spectra

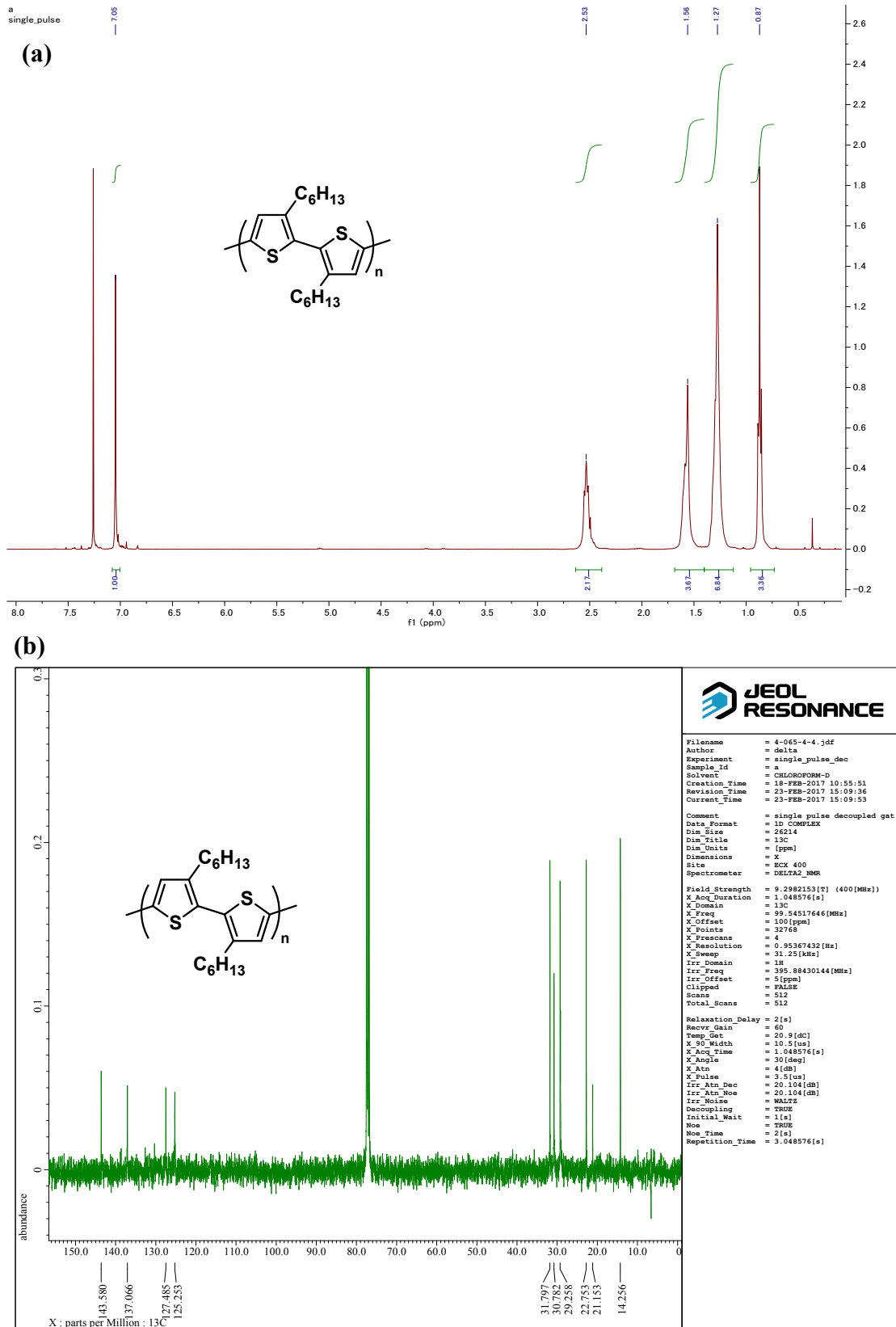


**Figure S1.** (a) <sup>1</sup>H NMR and (b) <sup>13</sup>C NMR spectra of HHTT-P3HT (Run 4).

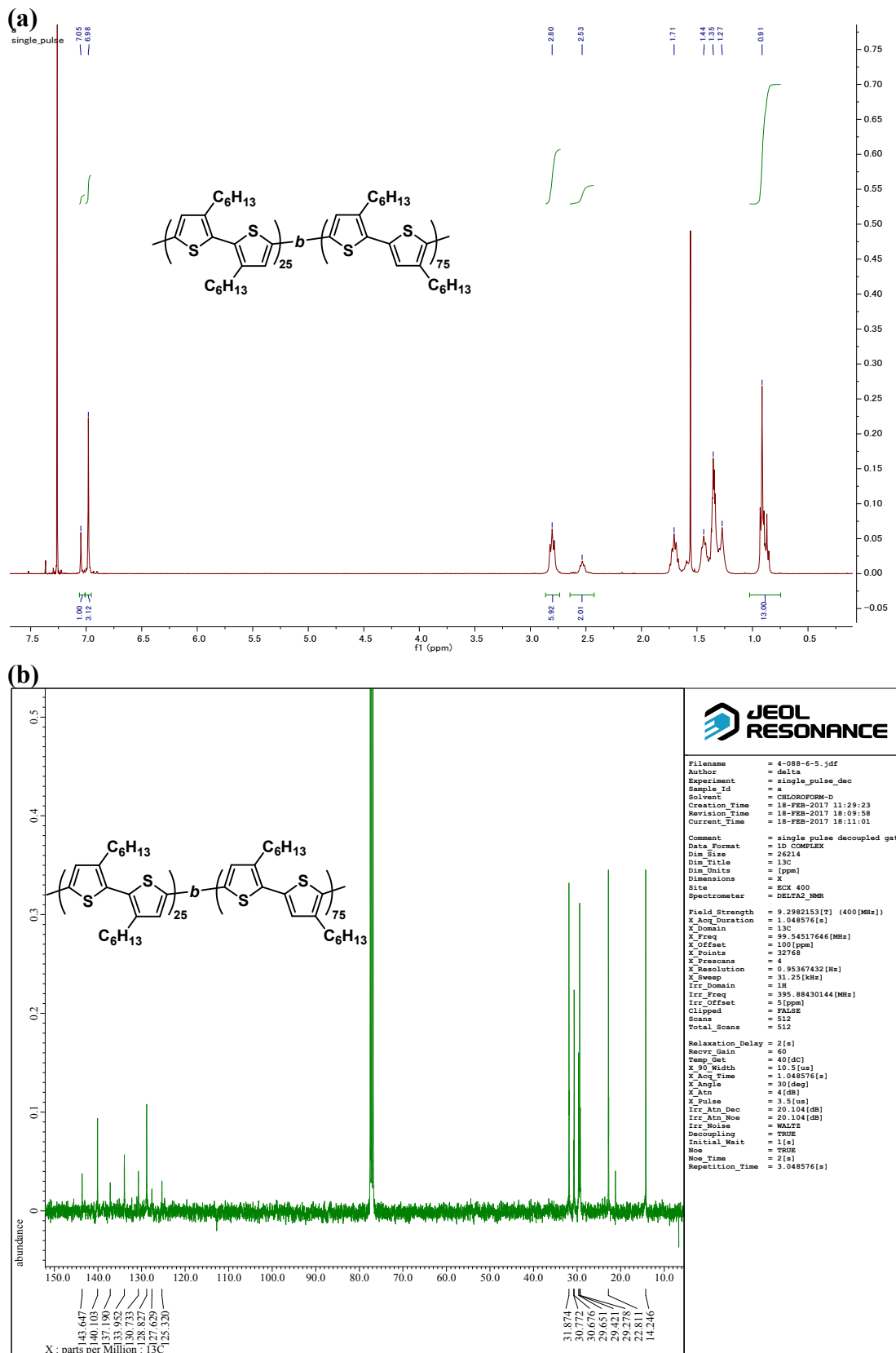


**Figure S2.** (a) <sup>1</sup>H NMR and (b) <sup>13</sup>C NMR spectra of regioblock P3HT (HHTT<sub>25</sub>HT<sub>75</sub>,

Run 6).

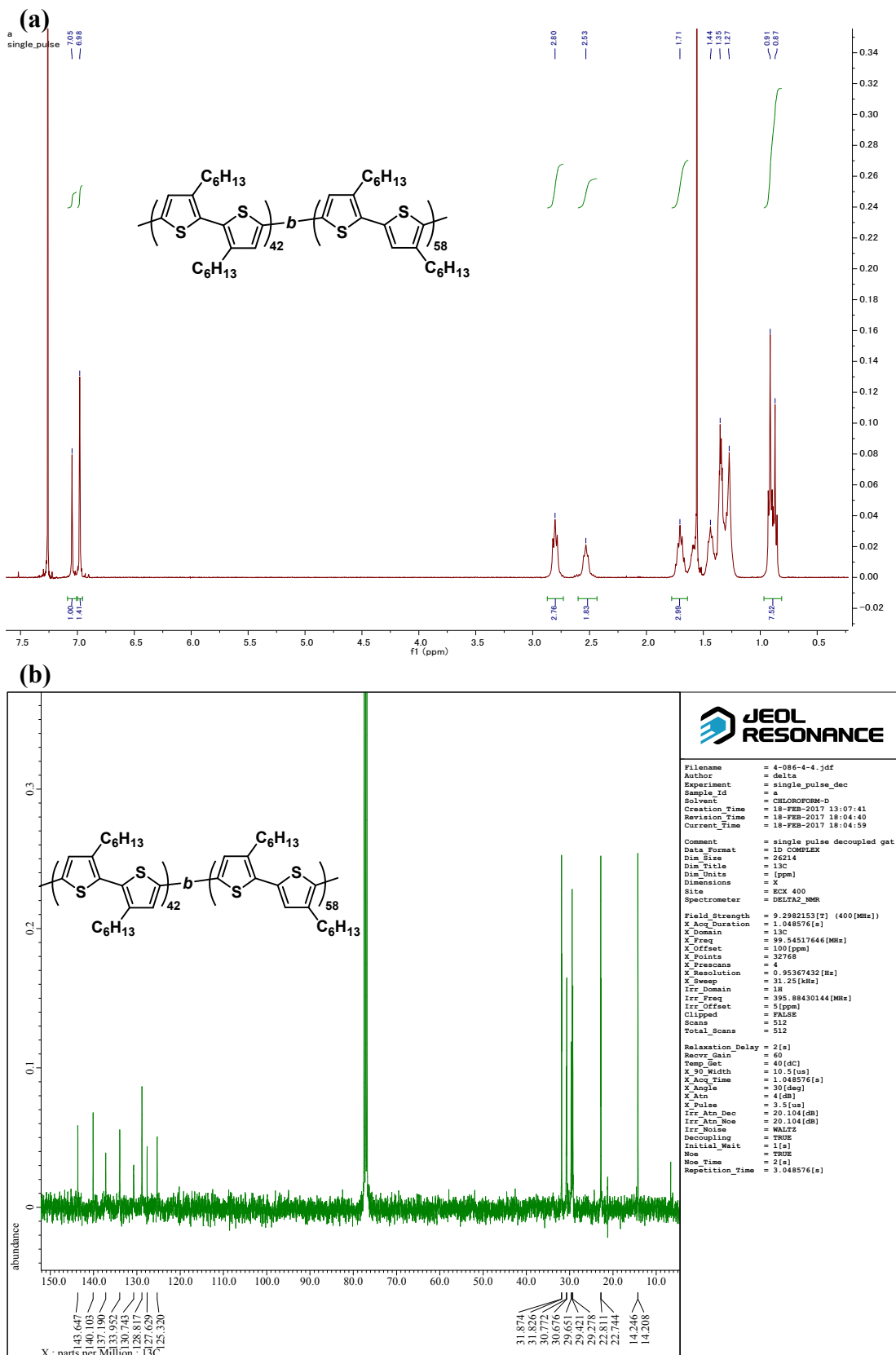


**Figure S3.** (a)  $^1\text{H}$  NMR and (b)  $^{13}\text{C}$  NMR spectra of regioblock P3HT (HHTT<sub>42</sub>HT<sub>58</sub>,

Run 7).

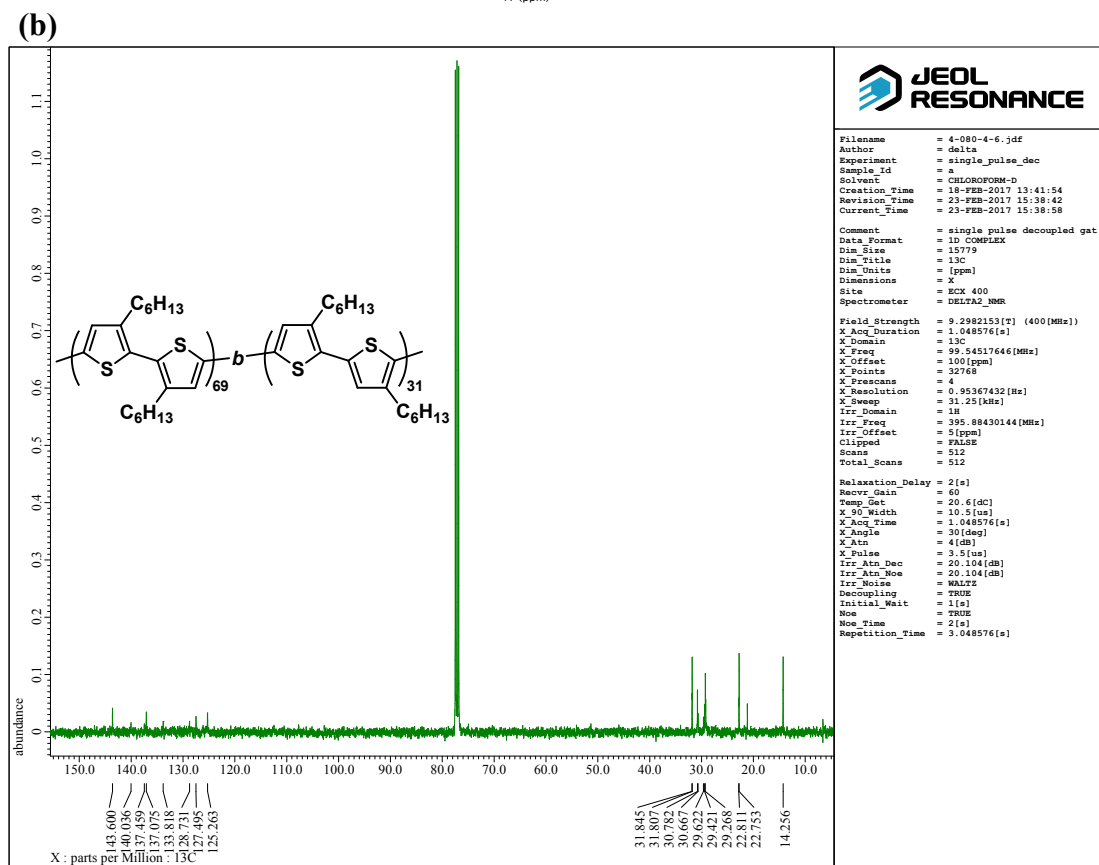
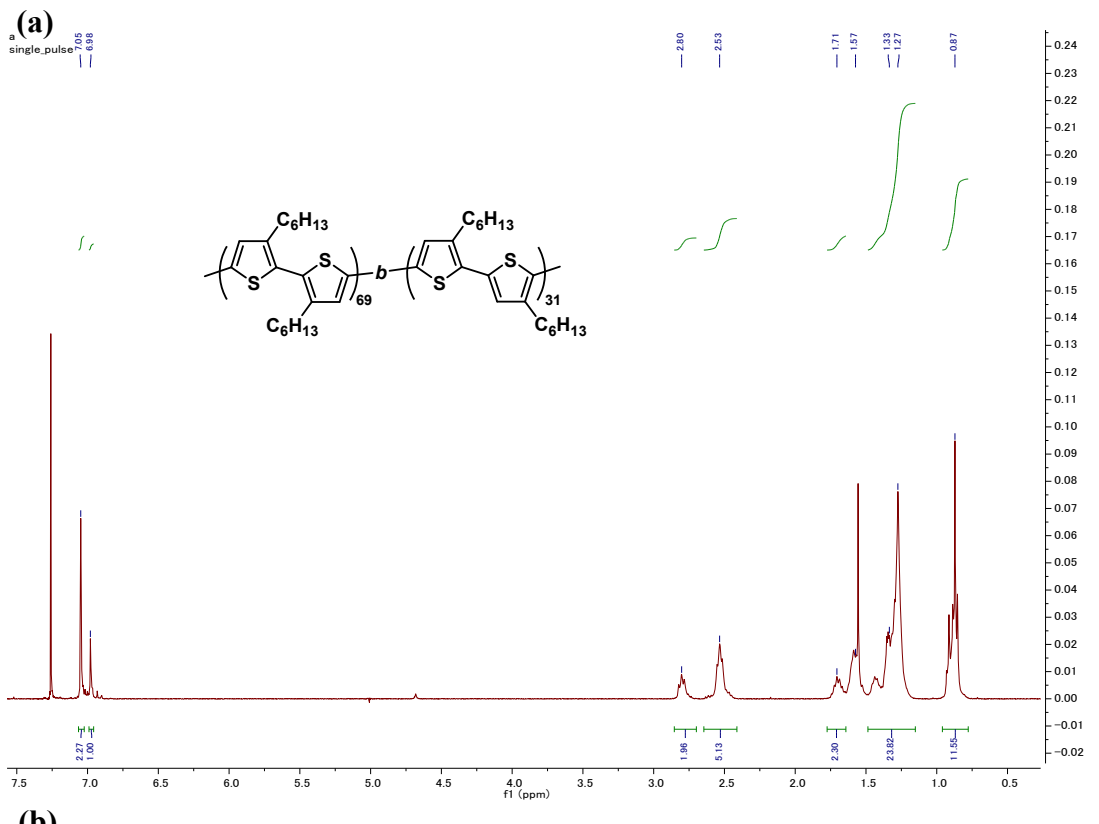


**Figure S4.** (a)  $^1\text{H}$  NMR and (b)  $^{13}\text{C}$  NMR spectra of regioblock P3HT (HHTT<sub>69</sub>HT<sub>31</sub>,

Run

8).

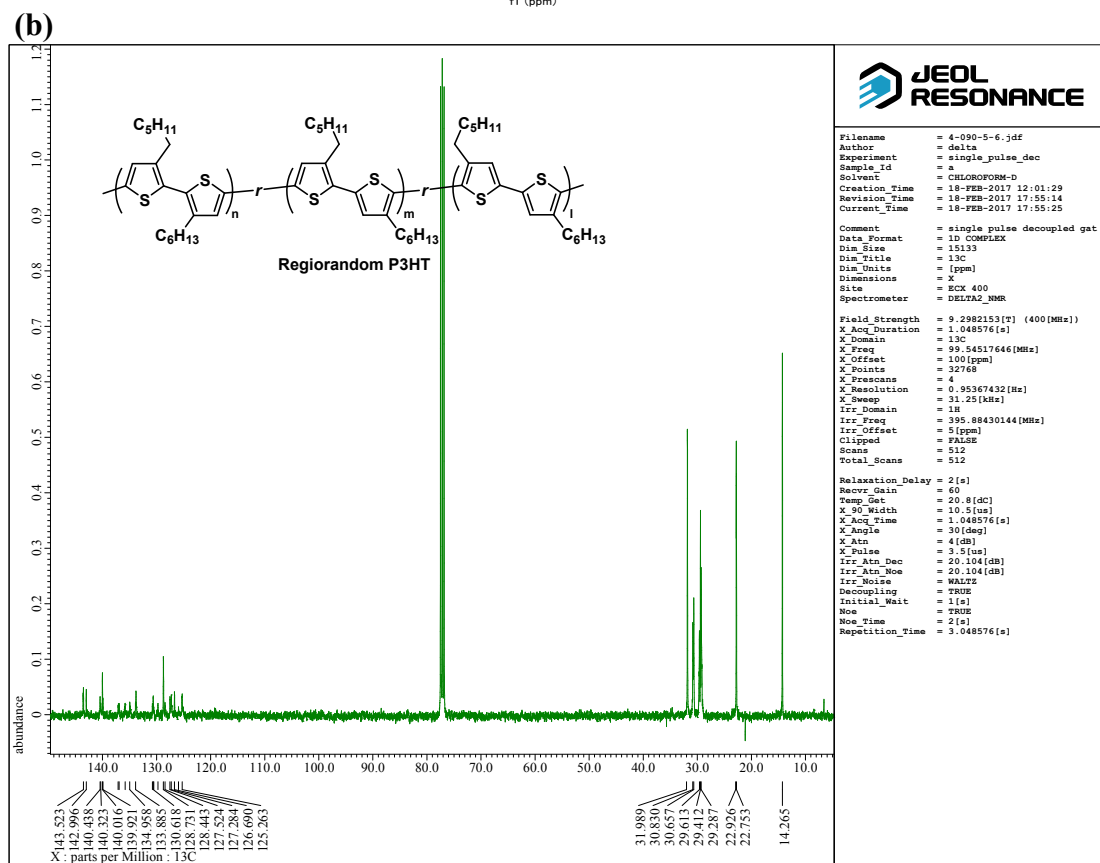
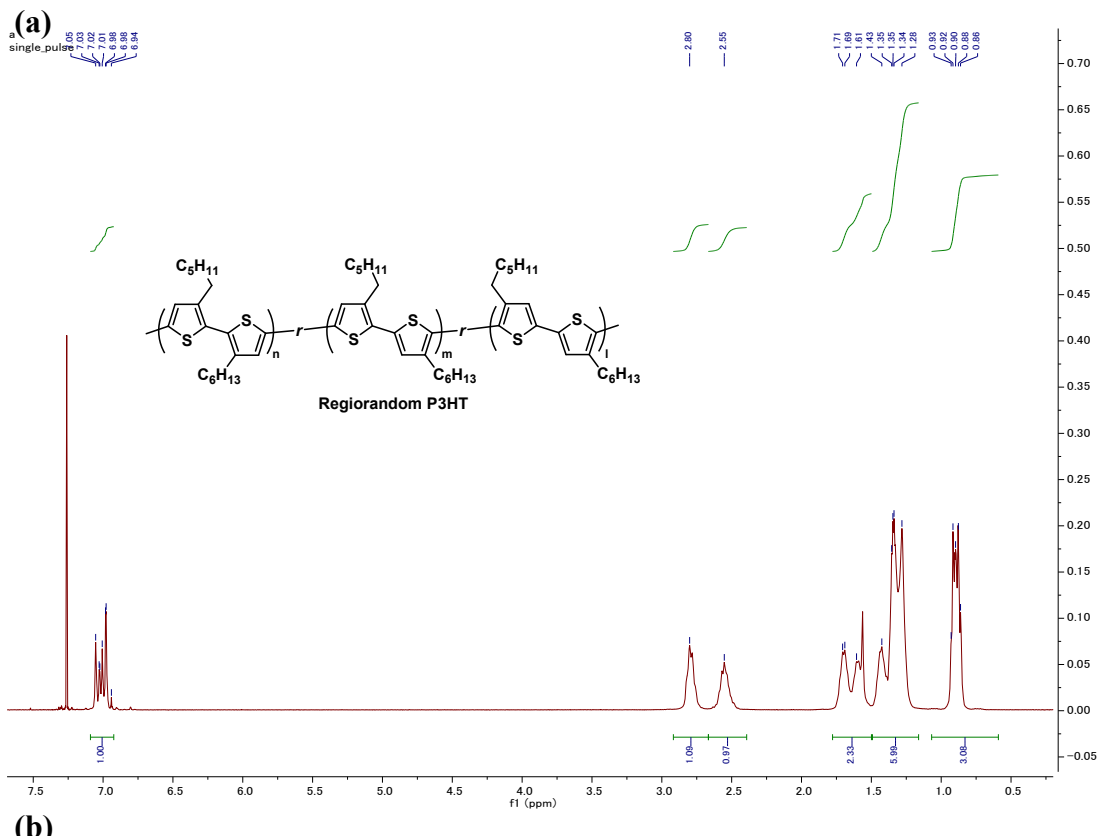
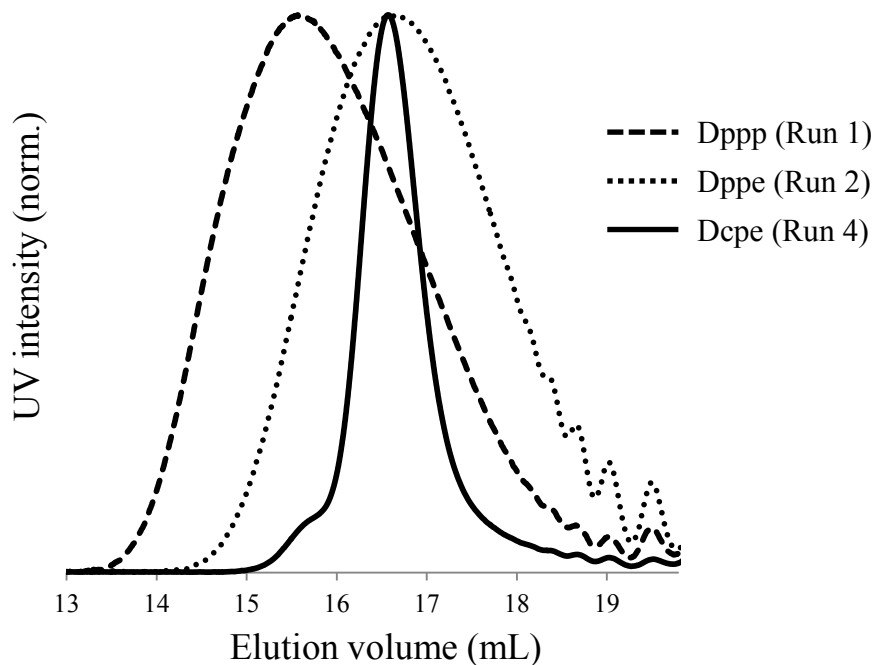


**Figure S5.** (a)  $^1\text{H}$  NMR and (b)  $^{13}\text{C}$  NMR spectra of regiorandom P3HT.

## SEC UV traces of HHTT-P3HT and regioblock P3HT

(a) Ligand effect



(b) Aiming different  $M_n$

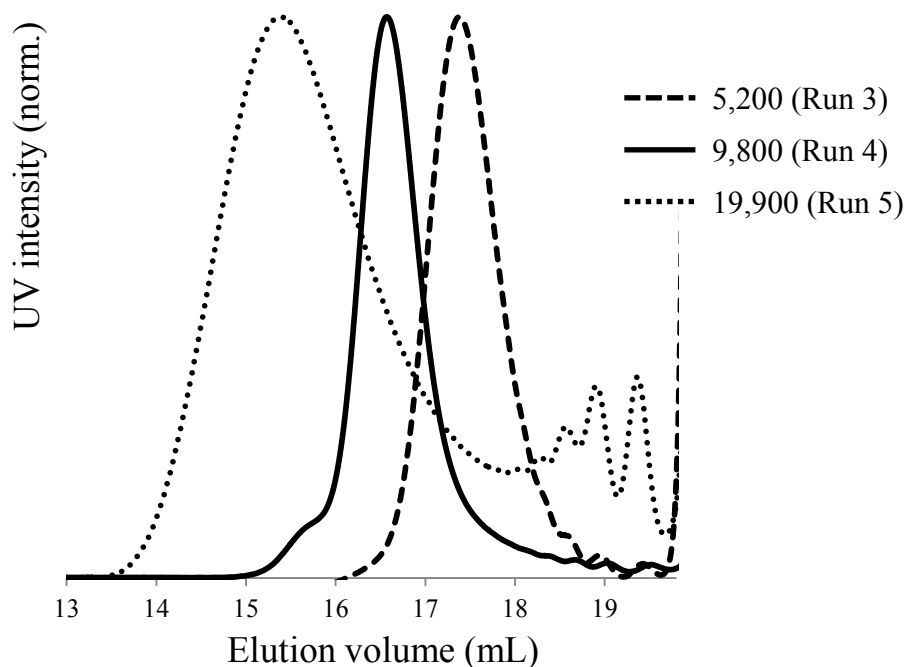


**Figure S6.** SEC UV traces of HHTT-P3HTs with (a) different ligands (Runs 1, 2 and 4) and (b) different [1]/ $\text{Ni}(\text{PPh}_3)_2\text{Cl}_2$  (Runs 3-5).

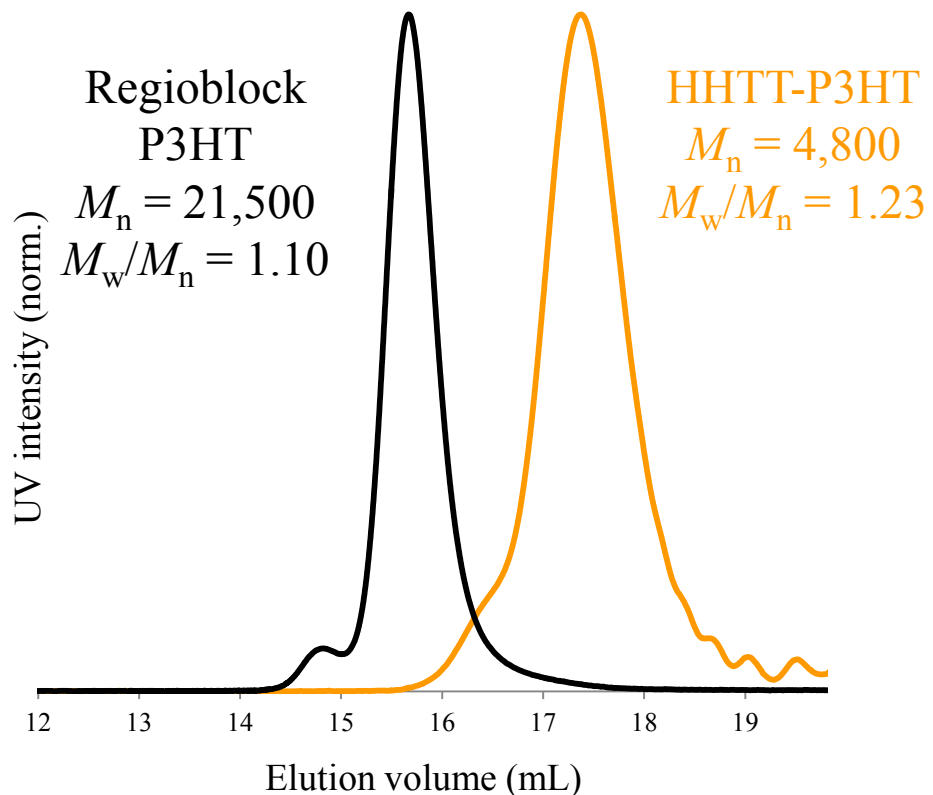


**Figure S7.** SEC UV traces of HHTT-P3HT (1<sup>st</sup> block, orange) and regioblock P3HT (HHTT<sub>25</sub>HT<sub>75</sub>, Run 6, black) after the successive addition of the HT-monomer (2<sup>nd</sup> block).

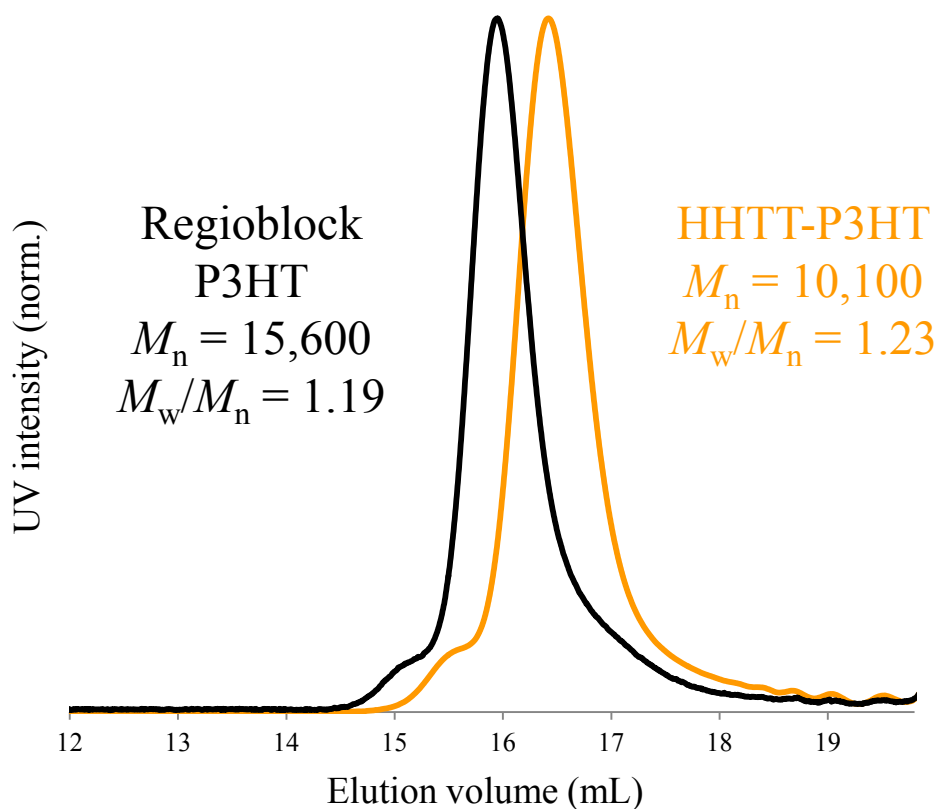


**Figure S8.** SEC UV traces of HHTT-P3HT (1<sup>st</sup> block, orange) and regioblock P3HT (HHTT<sub>69</sub>HT<sub>31</sub>, Run 8, black) after the successive addition of the HT-monomer (2<sup>nd</sup> block).

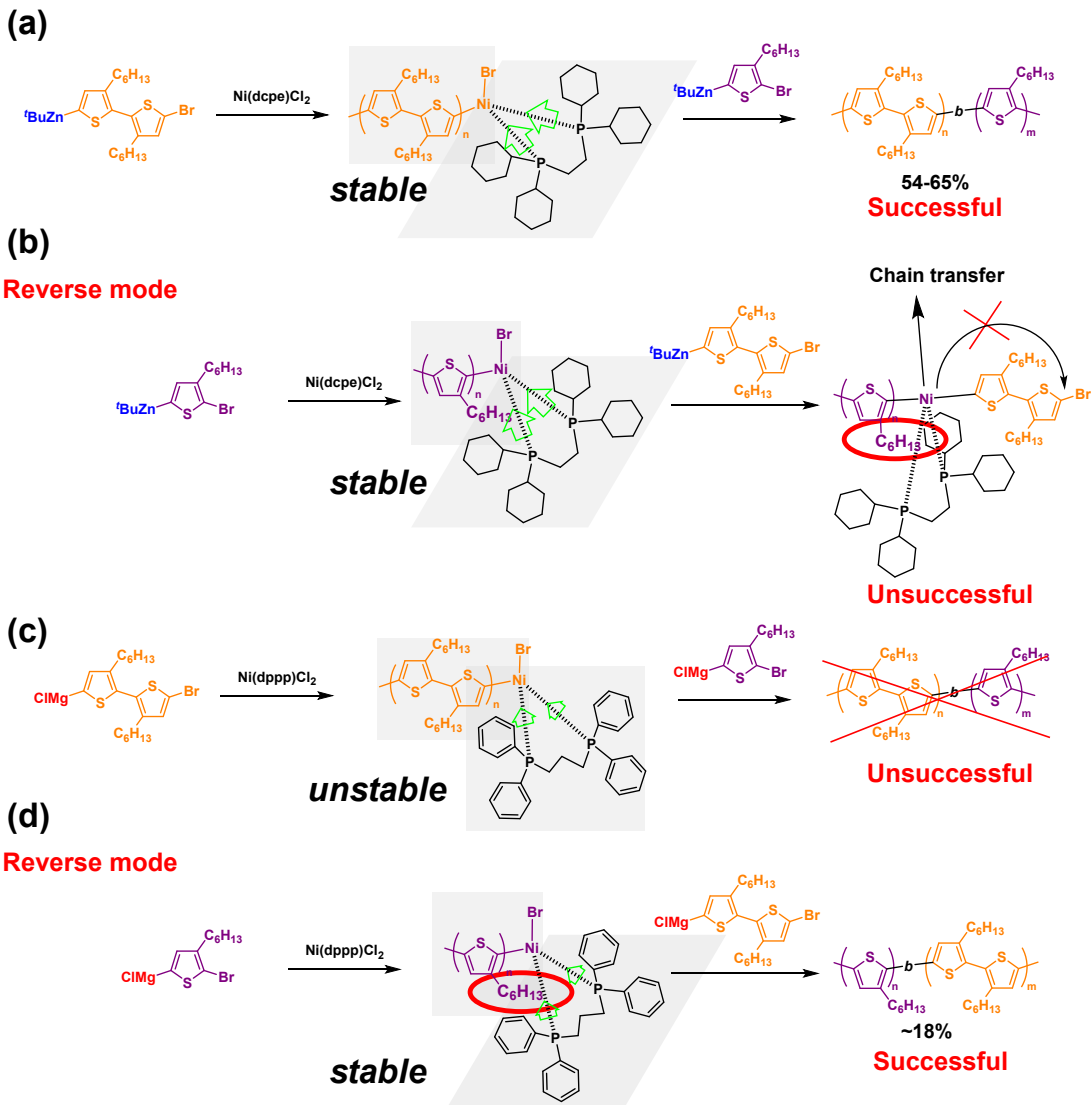


**Figure S9.** Schematic illustrations of plausible structures/mechanisms for (a) successful and (b) unsuccessful monomer addition sequences in NCTP and (c) unsuccessful and (d) successful monomer addition sequences in the conventional KCTP<sup>1</sup> for the synthesis of regioregular copolythiophenes.

## In-plane 1D GIWAXS profiles

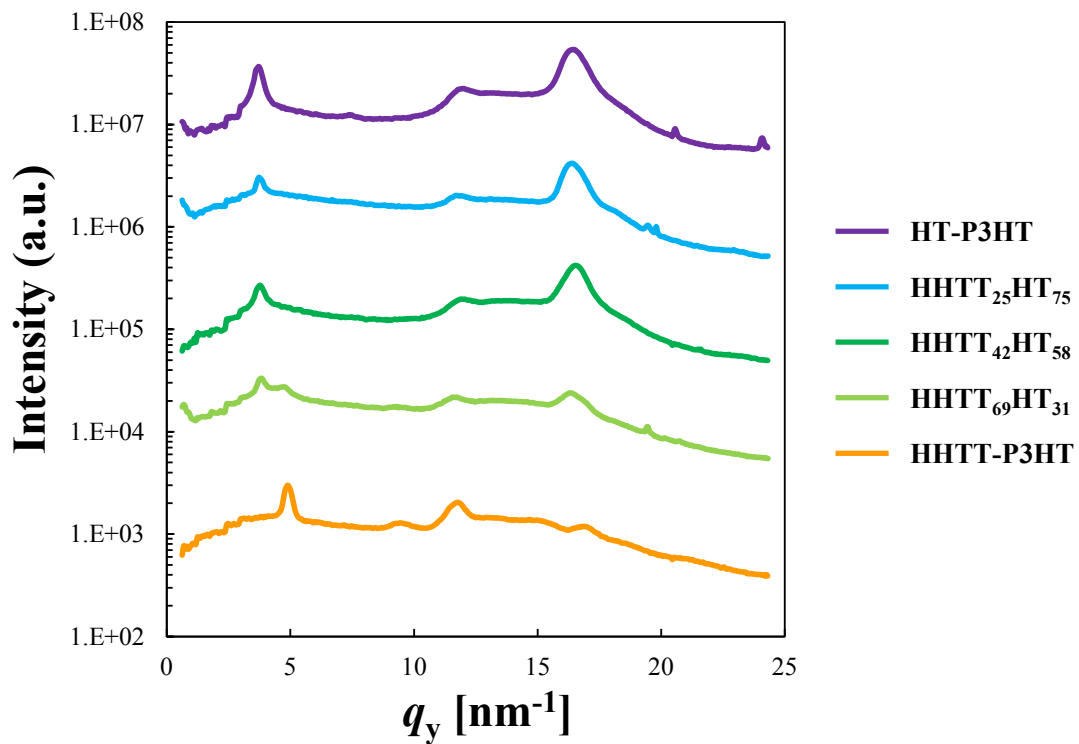


**Figure S10.** In-plane 1D GIWAXS profiles of HT-P3HT, HHTT<sub>25</sub>HT<sub>75</sub>, HHTT<sub>42</sub>HT<sub>58</sub>, HHTT<sub>69</sub>HT<sub>31</sub> and HHTT-P3HT. All of the films were spin-casted on a Si wafer and annealed at 150 °C for 1 h under vacuum.

## 2D GISAXS patterns

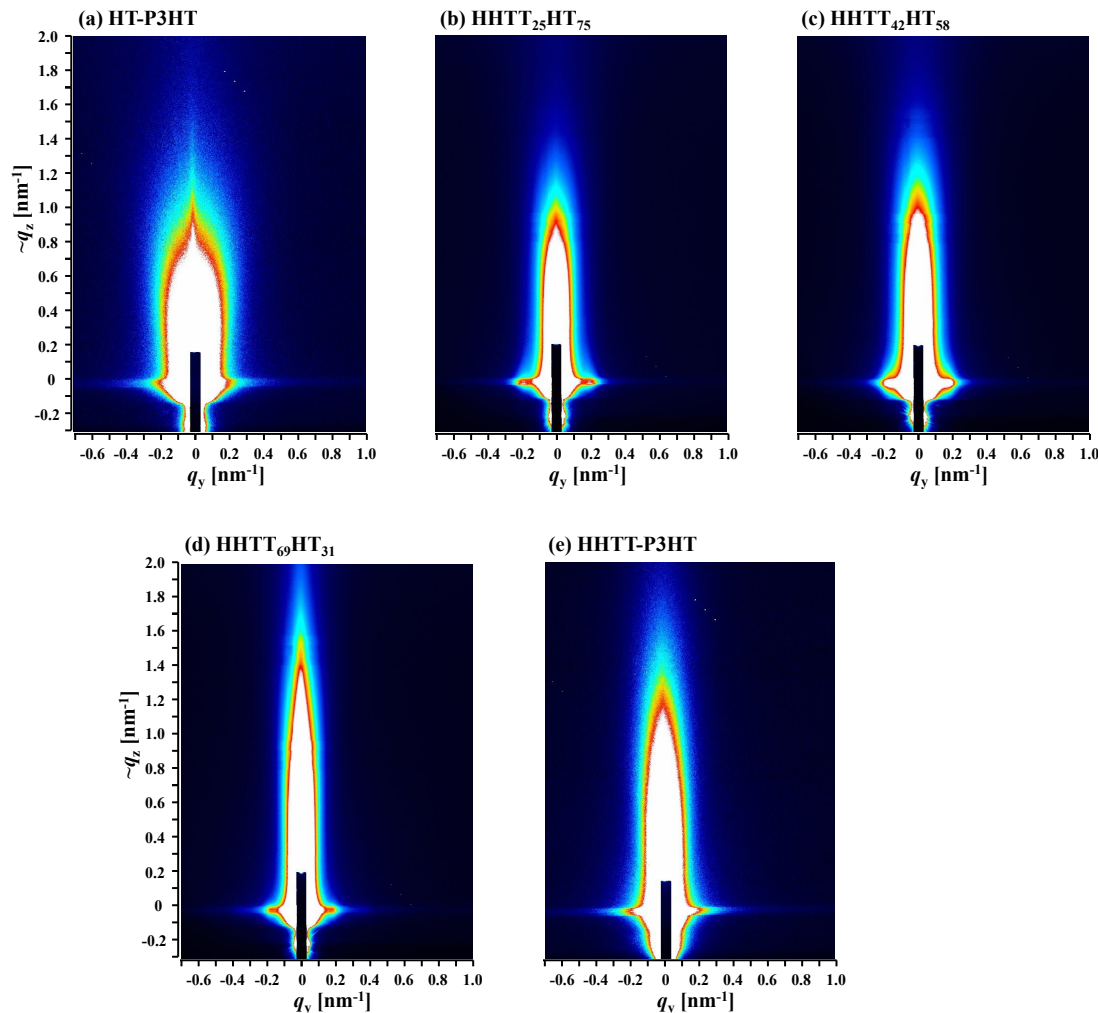


**Figure S11.** 2D GISAXS patterns of (a) HT-P3HT, (b) HHTT<sub>25</sub>HT<sub>75</sub>, (c) HHTT<sub>42</sub>HT<sub>58</sub>, (d) HHTT<sub>69</sub>HT<sub>31</sub> and (e) HHTT-P3HT. All of the films were spin-casted on a Si wafer and annealed at 150 °C for 1 h under vacuum.

## Temperature dependency of in-plane 1D GISAXS profiles

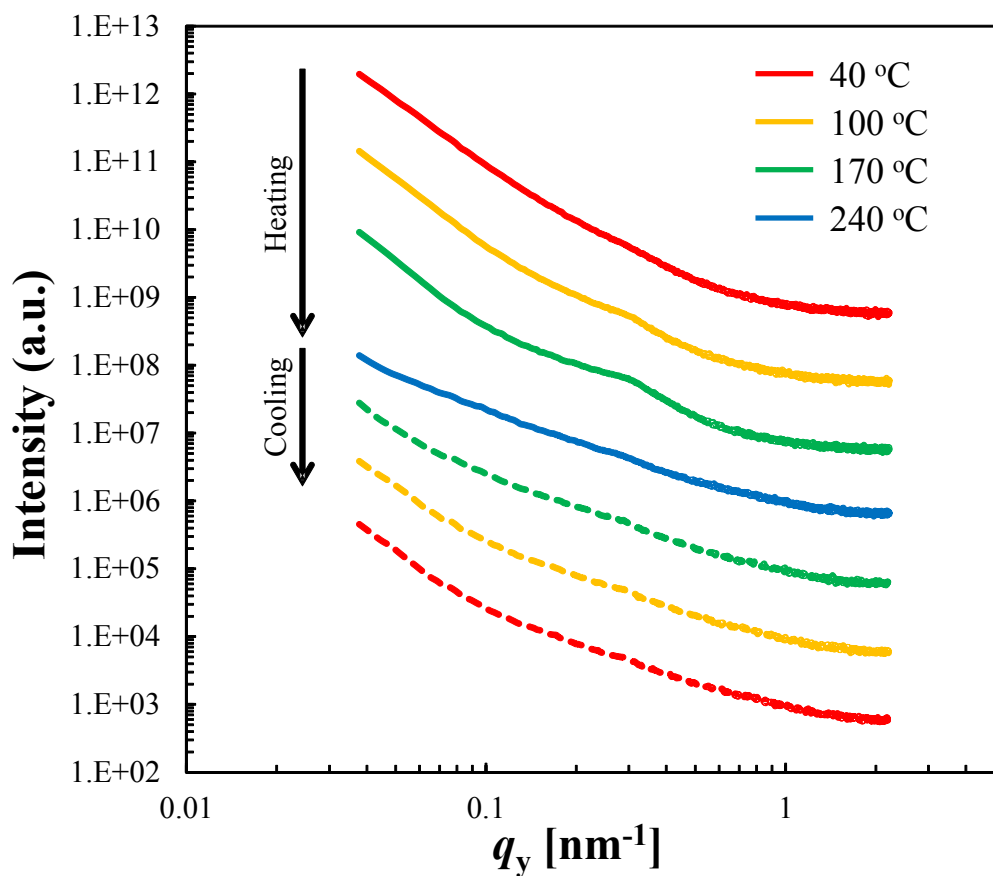


**Figure S12.** Temperature dependency of in-plane 1D GISAXS profiles of regioblock P3HT (HHTT<sub>42</sub>HT<sub>58</sub>, Run 7). The film was spin-casted on a Si wafer and heated up and cooled down gradually.

## TGA thermograms

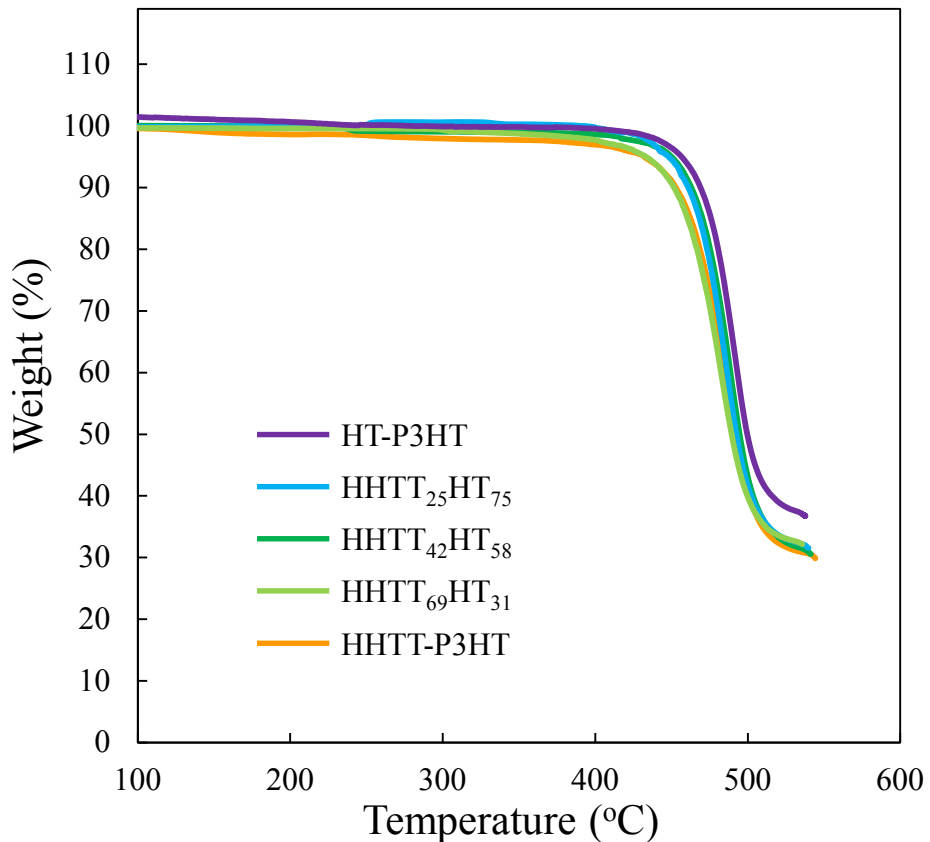


**Figure S13.** TGA curves of HT-P3HT, HHTT<sub>25</sub>HT<sub>75</sub>, HHTT<sub>42</sub>HT<sub>58</sub>, HHTT<sub>69</sub>HT<sub>31</sub> and HHTT-P3HT at the heating scan rate of 10 °C/min in N<sub>2</sub>.

## DSC thermograms

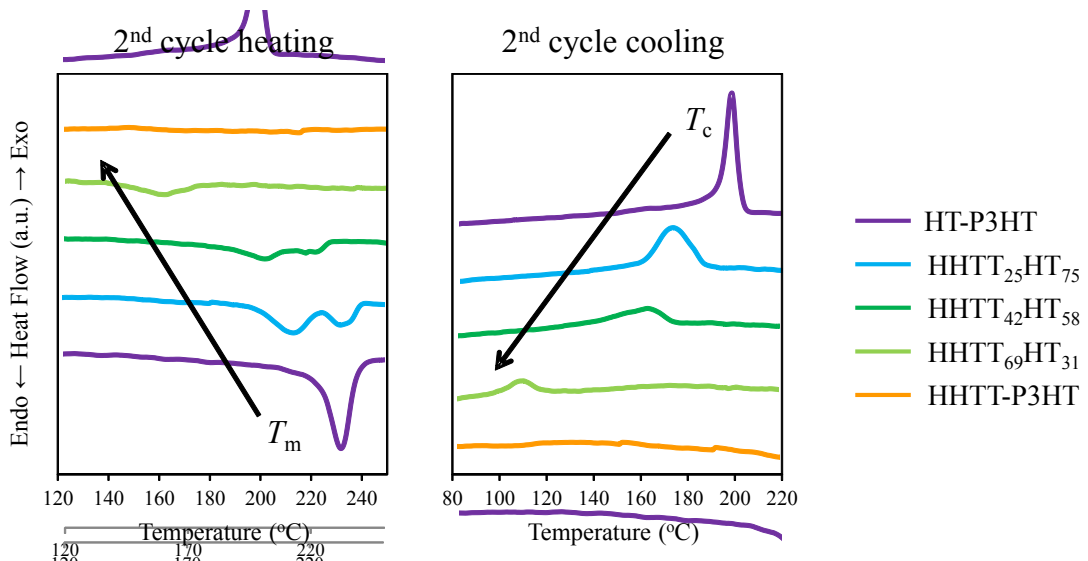


**Figure S14.** DSC curves at the 2<sup>nd</sup> cycle heating and 2<sup>nd</sup> cycle cooling scans of HT-P3HT, HHTT<sub>25</sub>HT<sub>75</sub>, HHTT<sub>42</sub>HT<sub>58</sub>, HHTT<sub>69</sub>HT<sub>31</sub> and HHTT-P3HT at the heating and cooling rate of 10 °C/min in N<sub>2</sub>.

**Table S2.** Thermal properties of HT-P3HT, HHTT-P3HT and regioregular P3HTs measured by TGA and DSC.

	$T_{d5\%}$ (°C) <sup>a</sup>	$T_m$ (°C) <sup>b</sup>	$\Delta H_m$ (J/g) <sup>c</sup>	$T_c$ (°C) <sup>b</sup>	$\Delta H_c$ (J/g) <sup>c</sup>	$X_c$ <sup>d</sup>
<b>HT-P3HT</b>	456	233.4	19.7	199.2	17.3	59.7
<b>HHTT<sub>25</sub>HT<sub>75</sub></b>	448	213.8	12.5	172.8	10.5	37.9
<b>HHTT<sub>42</sub>HT<sub>58</sub></b>	450	201.6	8.57	163.9	4.98	26.0
<b>HHTT<sub>69</sub>HT<sub>31</sub></b>	434	160.4	2.74	107.9	2.40	8.30
<b>HHTT-P3HT</b>	432	-	-	-	-	-

<sup>a</sup> The 5% weight-loss temperatures were evaluated by TGA at 10 °C/min in N<sub>2</sub>. <sup>b</sup> The melting and crystallizing temperature were evaluated by DSC at 10 °C/min in N<sub>2</sub>. <sup>c</sup> The melting and crystallizing enthalpies were evaluated from the integrated peaks of DSC. <sup>d</sup> Crystallinities were calculated from the comparison between evaluated  $\Delta H_m$  and an ideal melting enthalpy (33 J/g)<sup>2</sup>.

## UV-vis absorption

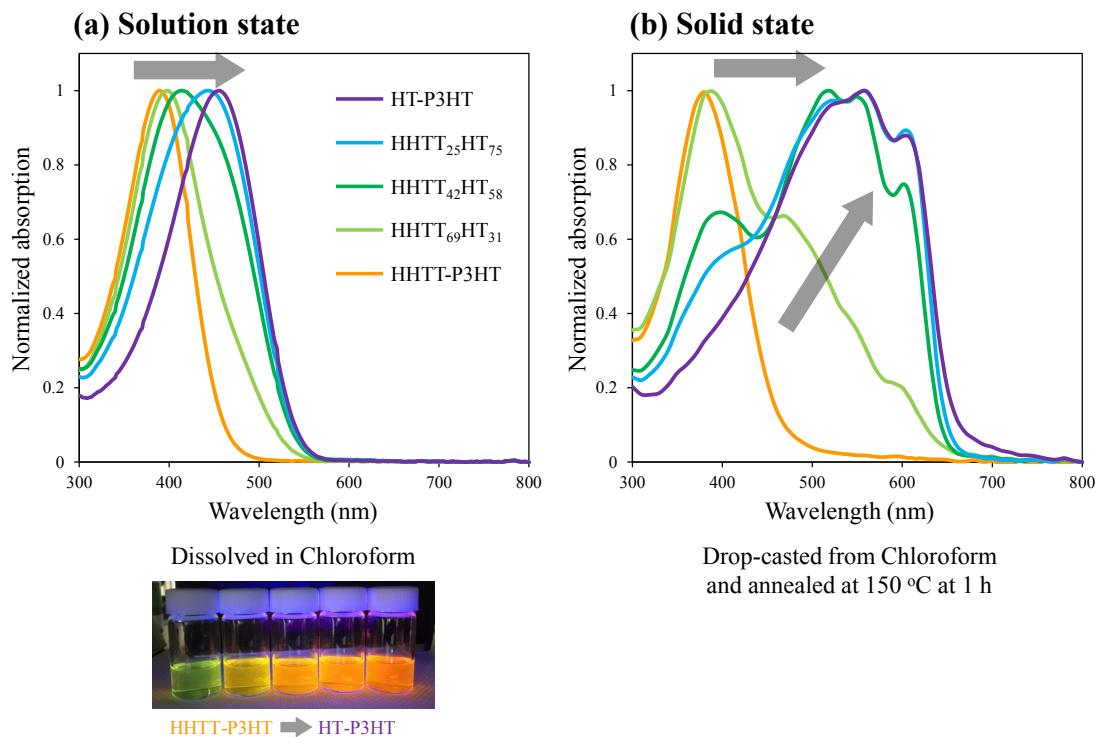


**Figure S15.** UV-vis absorption spectra of HT-P3HT, HHTT<sub>25</sub>HT<sub>75</sub>, HHTT<sub>42</sub>HT<sub>58</sub>, HHTT<sub>69</sub>HT<sub>31</sub> and HHTT-P3HT (a) dissolved in chloroform and (b) drop-casted from chloroform and annealed at 150 °C at 1 h under vacuum.

## Reference

- 1 X. Li, P. J. Wolanin, L. R. Macfarlane, R. L. Harniman, J. Qian, O. E. C. Gould, T. G. Dane, J. Rudin, M. J. Cryan, T. Schmaltz, H. Frauenrath, M. A. Winnik, C. F. J. Faul and I. Manners, *Nat. Commun.*, 2017, **8**, 15909.
- 2 J. Balko, R. H. Lohwasser, M. Sommer, M. Thelakkat and T. Thurn-Albrecht, *Macromolecules*, 2013, **46**, 9642–9651.